The use of continuum models for analyzing adobe structures

N. Tarque
Pontificia Universidad Católica del Perú, Peru
ROSE School, Istituto Universitario di Studi Superiori di Pavia, Italy

G. Camata & E. Spacone
Universita degli Studi 'Gabriele d'Annunzio' Chieti –Pescara, Italy

M. Blondet
Pontificia Universidad Católica del Perú, Peru

H. Varum
Universidade de Aveiro, Portugal

SUMMARY:
As it is known, the adobe structures have a high seismic vulnerability principally due to the low material strength and sometimes due to the inadequate structural configuration. One way for understanding the seismic behaviour of these structures is by experimental tests. However, those are costly and sometimes not easy to make. An alternative for this is the analysis of adobe structures by numerical tools with the possibility to make parametric studies for understanding the behaviour of different geometrical configurations.

In a previous work, some adobe material parameters have been calibrated based on a cyclic in-plane test. In this paper, that work was extended to a numerical modelling of the non-linear dynamic behaviour of an adobe module experimentally tested at the Pontificia Universidad Católica del Perú. For this, a continuum model in the finite element program Abaqus/Explicit, was used to represent the adobe masonry as a homogeneous and isotropic material.

Keywords: adobe, non-linear dynamic analysis, finite element, damaged plasticity based model

1. INTRODUCTION

Adobe constructions have some attractive characteristics, such as low cost, local availability, self/owner-made or no need for skilled labour (hence the name "non-engineered constructions"), good thermal insulation and acoustic properties (Memari and Kauffman 2005). However, adobe constructions do not perform well under seismic excitation and for this reason they are vulnerable in earthquake-prone regions. Thus, in order to improve their dynamic performance and to reduce the seismic vulnerability, it is important to study their seismic behaviour through experimental and numerical analyses. The biggest challenge to model properly the adobe constructions is the correct characterization of the material properties (especially in the inelastic range) and the correct geometric description of the structural components. Some inelastic material properties cannot be found experimentally; therefore, it is important to calibrate them numerically in order to describe properly the seismic behaviour of adobe constructions (Tarque 2011).

Adobe walls, as other type of masonry walls, have a very low tensile strength, thus cracks typically initiate in zones subjected to higher tensile stresses, such as corners of doors and windows. Usually, vertical cracks start at the connection of perpendicular walls, allowing the separation of them, due to the lack of confinement elements. Furthermore, horizontal cracks may form close to the façade base allowing it to overturn due to out-of-plane forces.

Masonry is a composite material formed by bricks and mortar joints. Each masonry component has its own material properties. Mortar is typically weaker and softer than the bricks. However, masonry
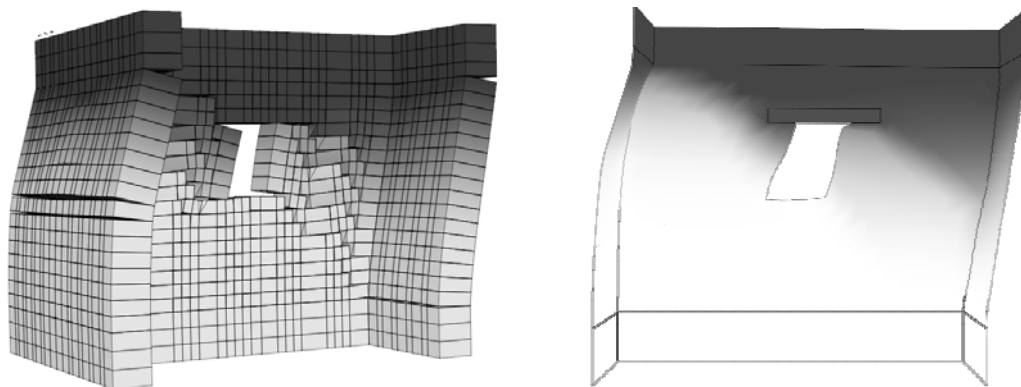
failure may also involve crushing and tensile fracturing of the masonry bricks and fracturing of the masonry joints (Stavridis & Shing 2010). In the case of adobe structures, the brick and mortar joints are made of similar materials, mainly soil. Therefore, as a first approximation, it seems reasonable to treat the adobe masonry as a homogeneous material.

This paper presents an attempt to capture the dynamic response and failure analysis of an adobe module using a nonlinear finite element model. For this, a continuum model called Concrete Damage Plasticity, which is implemented in the finite element program Abaqus/Explicit, was used to represent the adobe masonry as a homogeneous and isotropic material.

2. ANALYSIS METHOD

2.1 Finite element modelling

The masonry material can be numerically modelled following a discrete or continuum mechanic approach (*e.g.* Lotfi and Shing 1994; Lourenço 1996; Ngo and Scordelis 1967; Roca *et al*. 2010). The first assumes that the damage is concentrated at specific zones to simulate the block-to-block and block-to-mortar interaction (Roca *et al*. 2010). Generally the inelasticity behaviour is concentrated at the mortar joints to represent tension, shear and compression failure of the masonry. In this case the unit blocks (bricks) and the joint mortar are modelled using different finite elements. If the failure mechanism is known and the crack path can be identified, the discrete model accurately represents the actual cracking observed in the tests (Figure 2.1 left). The second approach, continuum model, predicts cracking and damage distributed all over the continuum, where a description of the interaction between bricks and mortar is not necessary since there is not physical difference between blocks and joint mortar (Figure 2.1 right). The crack propagation is mainly controlled by the shape of the constitutive law diagram and the material fracture energy (Cruz *et al.* 2004). Another approach consists in idealizing the structure through an equivalent frame where each wall is discretized by a set of masonry panels (piers and spandrels) in which the non-linear response is concentrated (*e.g.* Calderini *et al*. 2009; Magenes and Della Fontana 1998; Gambarotta and Lagomarsino 1997a; Galasco *et al*. 2004; Lagomarsino *et al*. 2007). The continuum modelling and the equivalent frame modelling are considered macro-modelling approaches; while the discrete approach is considered as part of the micro-modelling.

a) Adobe wall analyzed with a discrete approach   b) Adobe wall analyzed with a continuum approach
Figure 1.1. Deformation patterns of the numerical models developed by Tarque et al. (2011) for simulating the in-plane response of an adobe wall under a monotonically applied wall top displacement.

The failure assessment of concrete and masonry structures is mainly dependent on the material constitutive laws (Feenstra and de Borst 1992; Feenstra and Rots 2001). Similarly to concrete, adobe masonry behaves well under compression, but can only resists low tensile stresses with a quite brittle post-peak tensile behaviour. Since the adobe bricks and the mortar are composed of mud, both can be assumed as a homogeneous and isotropic material.

The adobe module examined in this paper was composed of adobe bricks, mud mortar, concrete foundation and a timber roof. The adobe bricks and the mud mortar were supposed to be a unique material and modelled with the concrete damaged plasticity model (continuum approach).

2.1.1 Continuum approach: the concrete damaged plasticity model
The concrete damaged plasticity model implemented in Abaqus/Explicit is developed for quasi-brittle materials subjected to cyclic loads and uses concepts of isotropic damaged elasticity in combination with isotropic tensile and compressive plasticity to represent the inelastic behaviour of the material. This model is based on the work developed by Lubliner *et al.* (1989) and by Lee and Fenves (1998), where the two main failure mechanisms are the tensile cracking and the compressive crushing of the material. This model assumes that failure of the material can be effectively modelled using its uniaxial tension, uniaxial compression and plasticity characteristics (Figure 2.2). In this work, an exponential and a parabolic curve have been selected for modelling the tension and the compression behaviour of the adobe material in the inelastic range, respectively (see Figure 4.2). The function parameters and the evaluation of the fracture energies are defined by Lourenço (1996) based on masonry tests; however, here those values were calibrated for adobe masonry.

The total strain is decomposed additively into the elastic and plastic strain, $\varepsilon = \varepsilon_e + \varepsilon_p$. Cracking in the plasticity-based model is represented by the damage factors, d_t and d_c, that reduce the elasticity module in tension and compression under reversal loads (Figure 2.2). When the material goes from tension to compression or viceversa, the parameters ω_c and ω_t controls the recovery of the compressive and tensile stiffness, respectively. The plastic deformation is defined as an irreversible process that dissipates energy as it proceeds.
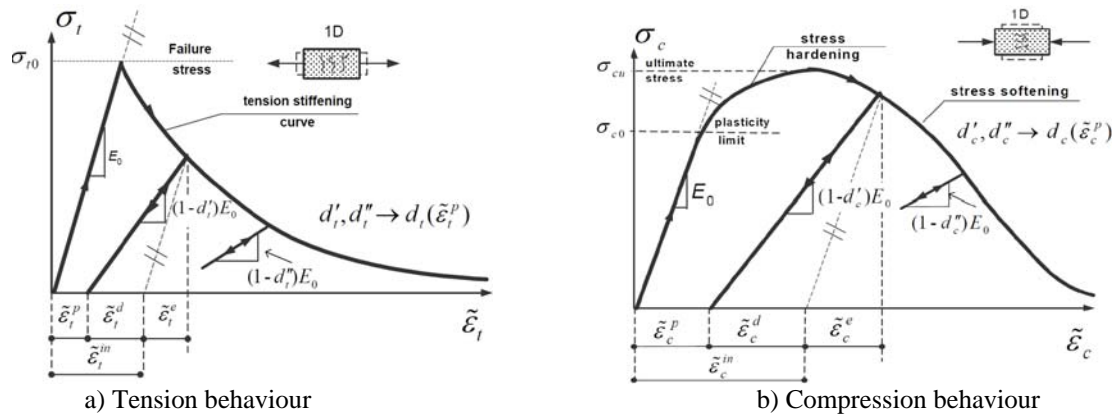

a) Tension behaviour   b) Compression behaviour
Figure 2.2. Model response under compression and tension loads implemented in Abaqus for the Concrete damaged plasticity model (modified from Wawrzynek and Cincio 2005).

3. EXPERIMENTAL TEST AT THE PONTIFICIA UNIVERSIDAD CATÓLICA DEL PERÚ

Blondet *et al.* (2006) carried out a dynamic test on an adobe module to analyze the seismic response and the damage pattern evolution on the adobe masonry. The unidirectional dynamic test was performed on an adobe module built over a reinforced concrete ring beam to facilitate the anchor of the specimen to the unidirectional shake table. The total weight (module + foundation) was around 135 kN. The weight of the concrete beam was 30 kN. The adobe bricks and the mud mortar used for the construction of the module had a soil/coarse sand/straw volume proportion of 5/1/1 and 3/1/1; respectively. The module consisted of four walls 3.21 m long, identified as North (N), South (S), East (E) and West (W) wall. The wall thickness of the north wall was 0.28 m because it had mud stucco, while the other walls had 0.25 m. wall thickness (Figure 3.1).

The longitudinal walls (parallel to the direction of the displacement signal) included a central window opening. The east wall had a door opening and the west wall did not have any openings. The roof consisted of wooden joists covered with cement tiles, the wooden were attached to the walls with steel

nails. The idea of the module was to represent a part of a typical vernacular Peruvian adobe building within the limitations of the 4.0x4.0 m shake table, which allows a maximum specimen weight of 160 kN.
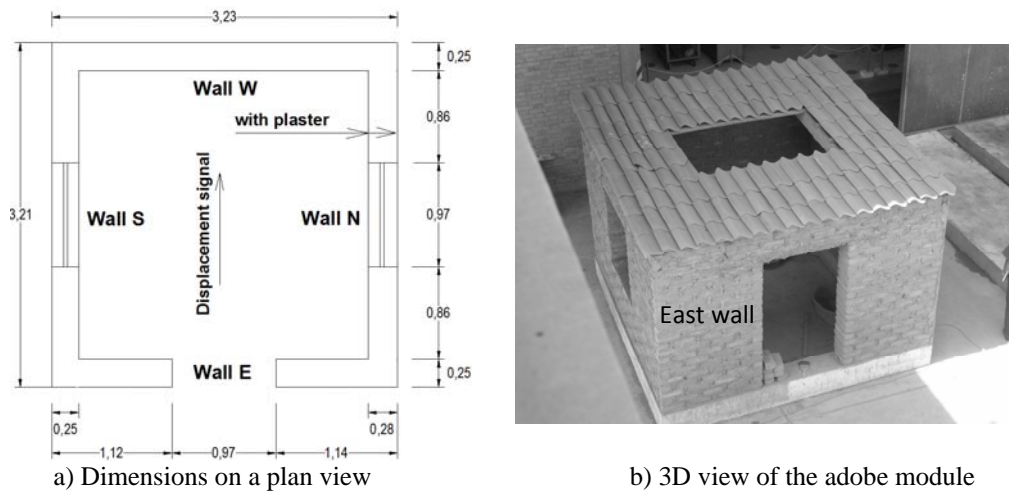

a) Dimensions on a plan view b) 3D view of the adobe module

Figure 3.1. Adobe module tested at the PUCP.

The adobe module was unidirectional subjected to three levels of displacement signals, which were scaled to have maximum displacements of 30, 80 and 130 mm at the base, the input displacement signals were related to PGA of 0.3, 0.8 and 1.2g, respectively. These earthquake levels (phases) intend to represent the effects of a frequently, moderate and severe earthquake on the adobe buildings. The displacement input was obtained and processed from the acceleration signal of the May 31st, 1970 earthquake recorded in Lima by the Peruvian Geophysics Institute (Figure 3.2). This earthquake was Mw 7.9 and occurred around 375 km far away from Lima.
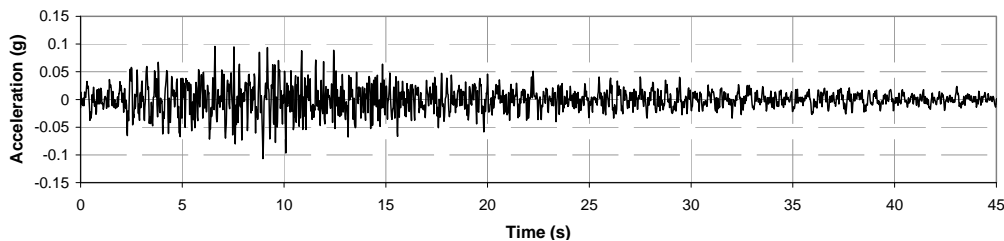

Figure 3.2. Horizontal EW acceleration record from the May 31st, 1970 earthquake recorded in Lima, Peru.

Ten accelerometers and 8 LVDT were left in the model distributed in all the walls, and 1 accelerometer and 1 LVDT were left at the shake table (Figure 3.3). The module was tested after more or less two weeks from the end of the construction.
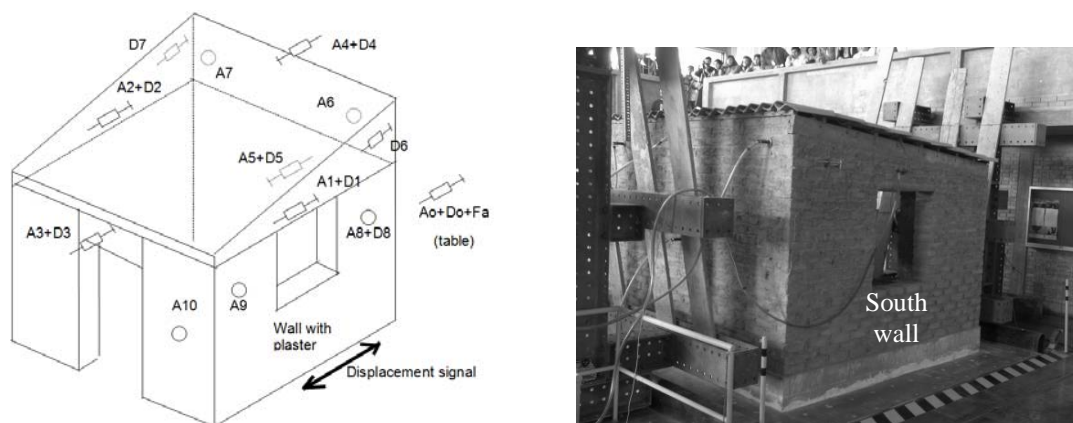

Figure 3.3. Disposition of the accelerometers and LVDTs on the adobe module.

3.1 Damage description

The displacement signals were applied parallel to the two walls with window (identified as North and South Wall). At the end of the Phase 1 and during the Phase 2 typical vertical cracks appeared at the wall intersections causing the separation of the walls; then, x-shape cracks appeared at the longitudinal walls, and cracks due to horizontal and vertical bending appeared at the transverse walls. The anchorage of the steel nails that connected the wooden beams with the walls was lost during the movement, and as a result the roof was supported by the walls just by its own weight and by friction. Major damage was observed during the second phase and a total collapse was observed during the third phase. The South Wall, which had stucco, was stiffer than the other walls. The difference in stiffness from the two parallel walls triggered torsional effects in the structure during the second and third phases. The displacement response of each wall is shown later in section 4.2.

The West Wall, which was itself broken more or less into 3 big blocks (typical of walls supporting just by three sides), had a rocking behaviour due to out-of-plane actions. During the third phase, which maximum displacement of 130 mm at the base, the perpendicular walls felt down at the beginning of the input signal while the parallel walls were completely cracked. Since the roof was supported by the lateral walls, it did not collapse. In this work the second phase was reproduced with the numerical model.

The vertical cracks at the wall intersections varied in thickness according to the amplitude of the signal. From the displacement histories reported by the LVDT during the phase 2, it was seen that all the walls have a maximum relative displacement right after 10 s of signal (see section 4.2), where the vertical cracks seemed to reach its maximum value. After this, the two walls parallel to the movement moved as a rigid body, while the two perpendicular walls moved back and forth within a rocking behaviour. The formation of vertical cracks made possible the separation of walls, allowing them to move independently. Besides, it can be seen from the displacement time history that after the walls separate from each other, the stiffer wall was the north wall (see Figure 4.5).

4. NUMERICAL STUDIES

4.1 Description of the model and material properties

A finite element model was created in Abaqus to simulate the non-linear dynamic response during the phase 2 of the adobe module presented before (Figure 4.1).
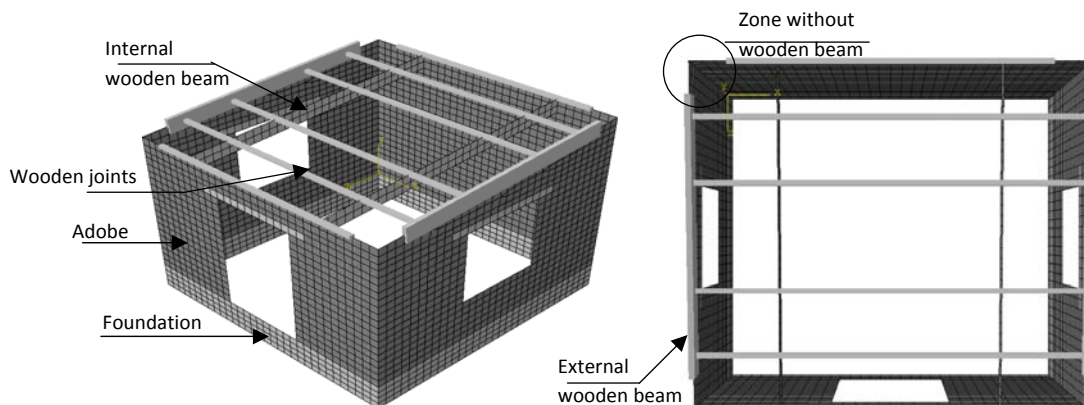

Figure 4.1. Finite element model of the adobe module built in Abaqus/Explicit.

The foundation (concrete ring beam), the adobe walls, the lintels and two internal wooden beams were represented by plane-stress shell elements. The other wooden beams (placed above the walls with windows) and the joints were modelled with beam elements. The foundation was fully fixed at the base during the application of gravity loads; after this, just one displacement DOF in the direction of

the movement was released in order to apply the acceleration at the base. The perimetral wooden beams were reduced in length to avoid a rigid connection between them; in this case, the walls could developed vertical cracks at the intersections without any additional restriction due to the ring beam (Figure 4.1 right). This model did not simulate the real interaction between the wooden beams and the adobe walls, since there was not enough information about the resistance of the steel nails inside the adobe bricks. The internal wooden beams were modelled using shell elements to distribute the stresses among more contact points between the beams and the perpendicular adobe walls, this avoided stress concentration.

The model consisted on 3406 nodes, 232 linear line elements B31, 3038 quadrilateral 4-nodes shell elements S4 (full integration), and 6 triangular 3-nodes shell elements S3 (full integration). All the walls had 5 Gauss integration points through the thickness. The thickness of the north wall was 280 mm and the thickness of the other walls was 250 mm. The mesh size was, in majority, kept as 100 x 100 mm, obtaining in this way a characteristic length h= 141.4 mm. The total mass of the model was 14.21 N.s^2/mm considering the concrete and wooden elements.

The concrete and the wooden materials were modelled elastically, whereas the adobe walls were modelled with the concrete damaged plasticity model. The material properties for adobe were the ones calibrated by Tarque (2011) and specified in Figure 4.2 and Table 4.1, Table 4.2, where E is the modulus of elasticity; υ is the Poisson's ratio, γ_m is the weight density, f_t is the tensile strength, G_f^I is the fracture energy for Mode I (related to the tensile softening), f_c is the compressive strength, G_f^c is the compressive fracture energy, and ε_p is the peak equivalent plastic strain. To represent the degradation of the elastic stiffness due to reversal loads, the following pairs of tensile damage factors (d_t) and tensile plastic displacements were assumed considering a characteristic length h= 141.4 mm: (0.00; 0.00), (0.85; 0.125), (0.90; 0.25), (0.95; 0.50). The stiffness recovery in compression, w_c, was 0.5 and in tension, w_t, was 0.0. Besides, the concrete damaged plasticity model requireed 4 more parameters for a complete description of the yield surface: the dilatancy angle, the eccentricity, the relation between the initial equibiaxial compressive yield stress to initial uniaxial compressive yield stress and a parameter that defines the shape of the yield surface in the deviatoric plane, these values were 1, 0.1, 1.16 and 2/3, respectively.
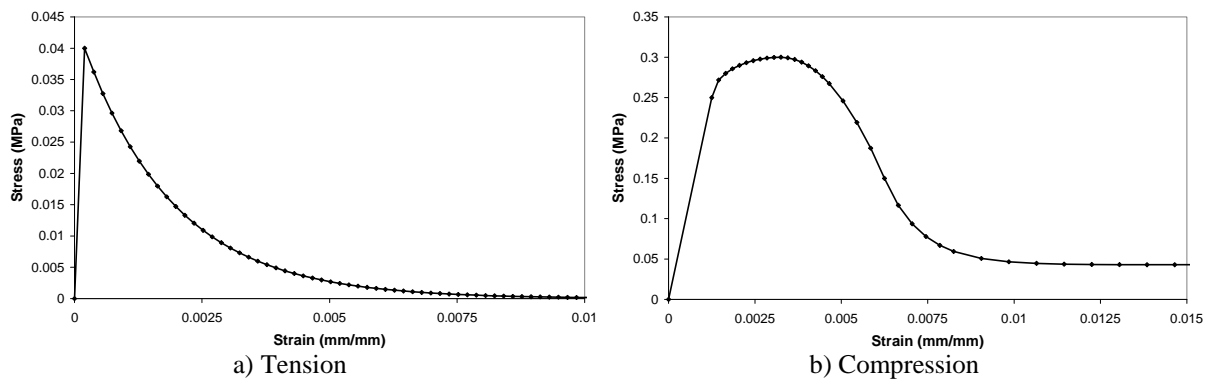

a) Tension   b) Compression

Figure 4.2. Constitutive laws for the adobe material.

Table 4.1. Elastic material properties of the adobe blocks, concrete and timber materials.

Concrete			Timber		
E (MPa)	υ	γ_m (N/mm^3)	E (MPa)	υ	γ_m (N/mm^3)
22000	0.25	2.4e-05	10000	0.15	6.87e-06

Table 4.2. Material properties for the adobe masonry within the concrete damaged plasticity model.

Elastic				Tension		Compression		
E (N/mm^2)	υ	γ_m (N/mm^3)	h (mm)	f_t (N/mm^2)	G_f^I (N/mm)	f_c (N/mm^2)	G_f^c (N/mm)	f_c (N/mm^2)
200	0.2	2e-05	141.4	0.04	0.01	0.45	0.155	0.40

4.2 Numerical results

The gravity load was applied using an implicit strategy in Abaqus/Standard. Afterwards, the results were loaded into Abaqus/Explicit and the horizontal acceleration was applied at the base. The numerical model reproduced just the Phase 2 of the experimental test. Abaqus/Explicit makes use of the central difference integration rule for integration of the equation of motions, which is more convenient when dealing with dynamic problems. The global stable time increment computed by Abaqus was 4.5018 e-06 s. Here it was assumed that the energy dissipation in the model was completely given by the hysteretic behaviour of the adobe material.

The crack pattern observed in the numerical results depicted fairly well the one observed in the experimental test: diagonal cracks appeared at the North and South walls, which were parallel to the movement, and cracks due to vertical and horizontal bending appear at the perpendicular walls: East and West walls. Figure 4.3 shows the tensile plastic strains of the numerical model at the end of the 30s acceleration signal. From the comparison of the two walls parallel to the movement, it was seen that the north wall was stiffer than the south wall due to the presence of the mud plaster. The no connection of the wooden beams at the corners allowed the development of vertical cracks at the wall intersections, so a rocking behaviour at the walls perpendicular to the movement could be simulated.
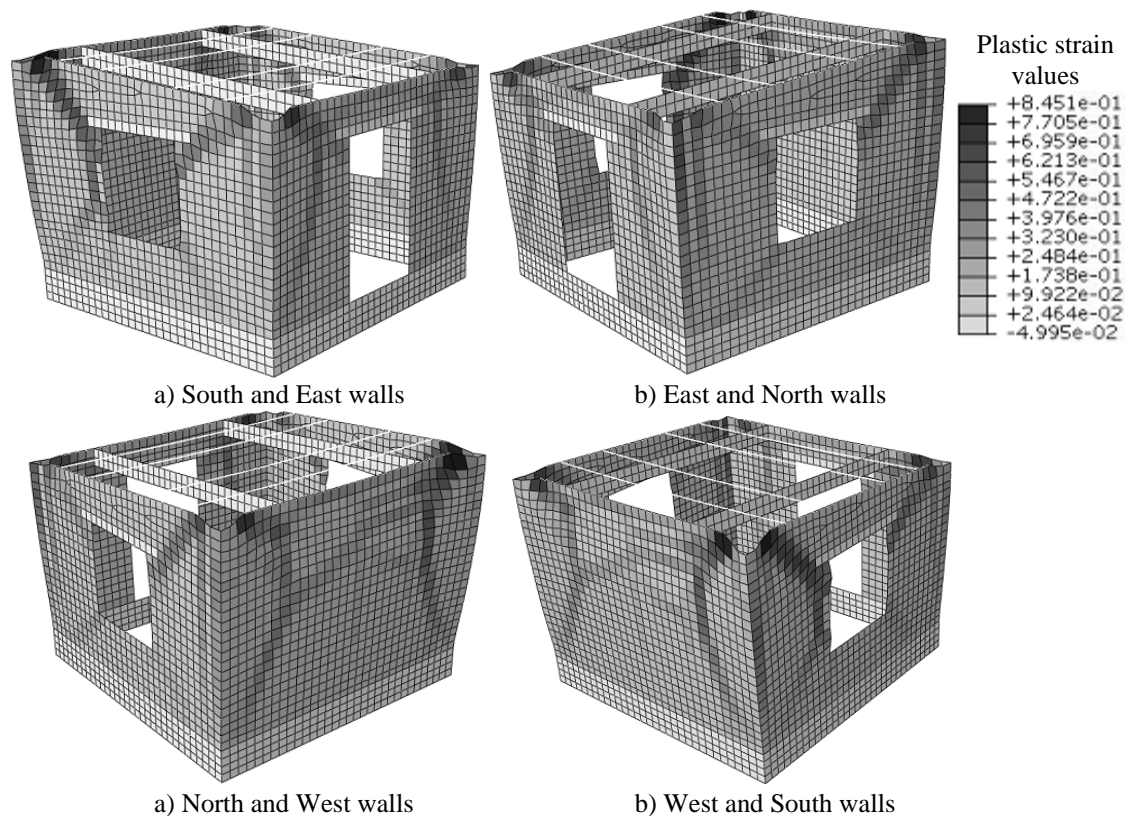

Plastic strain values
+8.451e-01
+7.705e-01
+6.959e-01
+6.213e-01
+5.467e-01
+4.722e-01
+3.976e-01
+3.230e-01
+2.484e-01
+1.738e-01
+9.922e-02
+2.464e-02
-4.995e-02

a) South and East walls   b) East and North walls

a) North and West walls   b) West and South walls

Figure 4.3. Tensile plastic strains of the numerical model built with concrete damaged plasticity in Abaqus/explictit.

Another way to see the zones were the adobe has already exceeded its tensile strength is by looking at the tensile damage factor plot (Figure 4.4). In this plot, the light colour represents the adobe zones which still behave elastically. The spandrels above the openings and the zones below the window openings got disconnected from the adobe walls and behaved almost elastically. The greater damage was seen at the intersection of the perpendicular walls and at the West wall, where stresses due to horizontal and vertical bending were the main source for its failure.
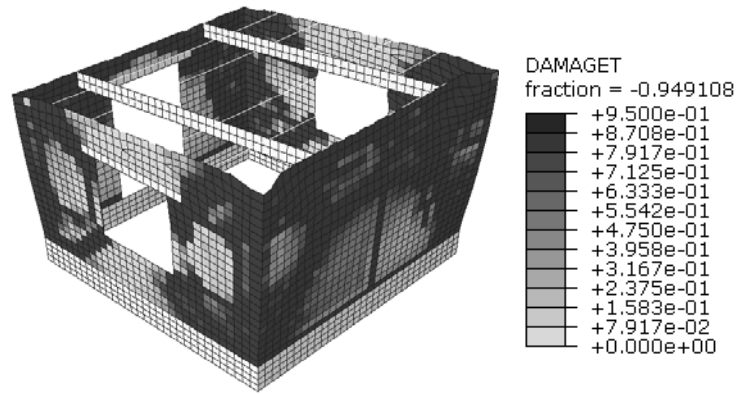
Figure 4.4. Tensile damage factor for numerical model at the end of the analysis in Abaqus/Explicit.

The numerical model gave good information about the cracking process, which can be used for retrofitting studies of adobe structures. The first cracks appeared vertically at the wall intersections. Then, vertical and horizontal cracks appeared at the perpendicular walls due to bending. As the movement continued, more diagonal cracking appeared at the walls with the formation of diagonal cracking at the parallel walls. After 10 s, where the big acceleration amplitudes were registered, the adobe walls presented complete damage. As it was said, the adobe masonry has poor tensile strength, so the identification of these zones under any ground acceleration was another advantage of having numerical models.

Figure 4.5 shows that the maximum relative displacement was around 10 s. Afterwards, the walls oscillated from a new equilibrium position indicating a residual inelastic displacement. The numerical rocking behaviour of the two walls perpendicular to the movement, in particular the out of plane displacement, differed from the experimental behaviour because this numerical model did not allow the elimination of the shell elements that reach the maximum tensile plastic strain, so it was not possible to obtain a completely independent behaviour between perpendicular walls. However, the model captured the failure and it was useful to understand the seismic behaviour of the adobe structure in terms of failure mechanisms. Figure 4.5 shows that the numerical relative displacement of the east and west walls depended on the relative displacements of the north and south walls, which were parallel to the movement.
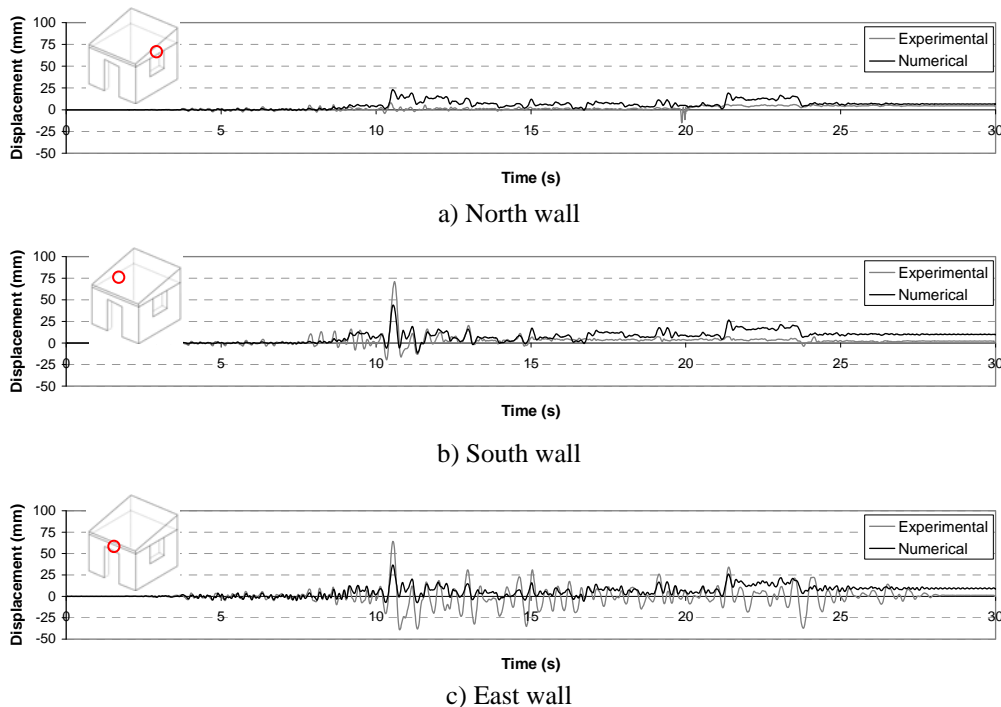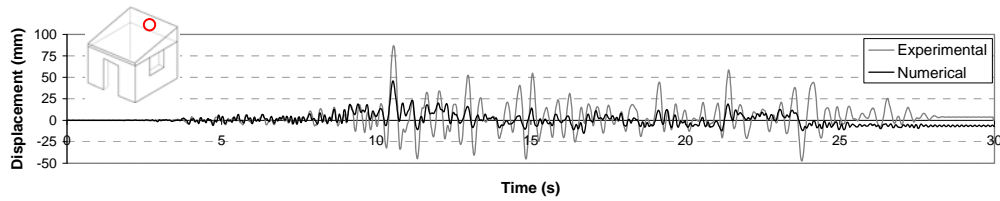

a) North wall

b) South wall

c) East wall

Figure 4.5. Experimental vs numerical displacement history of the adobe walls measured at the top.

d) West wall

Figure 4.5. Continuation. Experimental vs numerical displacement history of the adobe walls measured at the top.

5. FURTHER RESEARCH

Future work should consider the numerical analysis of reinforced adobe walls. Recently, Blondet *et al*. (2006) has experimentally evaluated the seismic capacity of adobe modules externally reinforced with polymer mesh. The results demonstrated a clear improvement in the global seismic capacity. The walls were broken into pieces but they did not collapse because the polymer mesh kept them together. The reinforcement system could be modelled as an isotropic material layer using Abaqus/Explicit placed at both sides of the adobe layer. After verify the efficiency of the numerical models, the methodology could be extended to the numerical analyses of earthen monuments.

6. CONCLUSIONS

This paper deals with the numerical non-linear dynamic analysis of an adobe module, previously tested at the Pontificia Universidad Católica del Perú by Blondet *et al.* (2006), following a continuum approach in Abaqus/Implicit and Abaqus/Explicit. The used constitutive model was the concrete damaged plasticity model, which assumed the adobe as an isotropic material. Besides, the adobe masonry can be considered as a homogeneous material represented by its tensile and compressive constitutive laws since the adobe and mortar are principally made of mud. The material properties (elastic and inelastic) were calibrated in a previous work by the authors (Tarque 2011) based on an experimental in-plane cyclic test on an adobe wall.

The numerical model was subjected to an acceleration record at the base related to the Phase 2 of the experimental test, which had a maximum base displacement of 80 mm. The numerical results represented fairly well the real crack pattern, failure mechanisms and displacement response, which validated the procedure following here for modelling the adobe module. To simulate the poor connection seen between the wooden beams of the roof and the adobe walls, the wooden beam elements were reduced in length to avoid a physical connection at the wall corners (see Figure 4.1 right).

The calibrated material properties proposed by the authors and the procedure for modelling adobe structures seen here are good enough for representing the non-linear dynamic response of adobe buildings under seismic excitations. This study can be extended to other adobe structure typologies in order to predict the seismic behaviour of different structural configurations and to evaluate possible strengthening solutions.

REFERENCES
Blondet, M., Vargas, J., Velásquez, J., and Tarque, N. (2006). Experimental Study of Synthetic Mesh Reinforcement of Historical Adobe Buildings, *Proceedings of Structural Analysis of Historical Constructions*, P. B. Lourenço, P. Roca, C. Modena, and Agrawal. S., eds., New Delhi, India, pp. 1-8.
Calderini, C., Cattari, S., and Lagomarsino, S. (2009). In plane seismic response of unreifnorced masonry walls: comparison between detailed and equivalent frame models, *ECCOMAS Thematic Conference on Computational Methods in Structural Dynamics and Earthquake Engineering*, M. Papadrakakis, N. D. Lagaros, and M. Fragiadakis, eds., Rhodes, Greece.

Cruz, J. S., Barros, J., and Azevedo, Á. (2004). Elasto-plastic multi-fixed smeared crack model for concrete, *Report 04-DEC/E-05*, University of Minho, Minho, Portugal.

Feenstra, P. H., and de Borst, R. (1992). The use of various crack models in F.E. analysis of reinforced concrete panels, *Proceedings of First International Conference on Fracture Mechanics of Concrete Structures: FraMCoS1*, Z. P. Bažant, ed., Taylor and Francis, Breckenridge, Colorado, USA.

Feenstra, P. H., and Rots, J. G. (2001). Comparison of Concrete Models for Cyclic Loading, *Modelling of Inelastic Behaviour of RC Structures under Seismis Loads*, P. Benson Shing and T.-aki Tanabe, eds., American Society of Civil Engineers, USA, pp. 38-55.

Galasco, Alessandro, Lagomarsino, Sergio, Penna, Andrea, and Resemini, S. (2004). Non-linear seismic analysis of masonry structures, *Proceedings of 13th World Conference on Earthquake Engineering*, Vancouver, Canada.

Gambarotta, L., and Lagomarsino, S. (1997). Damage models for the seismic response of brick masonry shear walls. Part II: The continuum model and its applications, *Earthquake Engineering & Structural Dynamics*, Vol. 26, No.4, pp. 441-462.

Lagomarsino, S, Galasco, A, and Penna, A. (2007). Non-linear macro-element dynamic analysis of masonry buildings, *Proceedings of ECCOMAS Thematic Conference on Computational Methods in Structural Dynamics and Earthquake Engineering*, Rethymno, Crete, Greece.

Lee, J., and Fenves, G. L. (1998). Plastic-Damage Model for Cyclic Loading of Concrete Structures, *Journal of Engineering Mechanics*, Vol. 124, No.8, pp. 892-900.

Lotfi, H. R., and Shing, P. Benson. (1994). Interface Model Applied to fracture of masonry Structures, *ASCE*, Vol. 120, No.1, pp. 63-80.

Lourenço, P. B. (1996). Computational strategies for masonry structures, *Ph.D. Thesis*, Delft University, Delft, The Netherlands.

Lubliner, J., Oliver, J., Oller, S., and Oñate, E. (1989). A plastic-damage model for concrete, *International Journal of Solids and Structures*, Vol. 25, No.3, pp. 299-326.

Magenes, G., and Della Fontana, A. (1998). Simplified non-linear seismic analysis of masonry buildings, *Proceedings of Fifth International Masonry Conference*, British Masonry Society, London, England.

Memari, A. M., and Kauffman, A. (2005). Review of Existing Seismic Retrofit Methodologies for Adobe Dwellings and Introduction of a New Concept, *Proceedings of SismoAdobe2005*, Pontificia Universidad Católica del Perú, Lima, Peru, p. 15.

Ngo, D., and Scordelis, A. C. (1967). Finite Element Analysis of Reinforced Concrete Beams, *American Concrete Institute*, Vol. 64, No.3, pp. 152-163.

Roca, Pere, Cervera, M., Gariup, G., and Pela', L. (2010). Structural Analysis of Masonry Historical Constructions. Classical and Advanced Approaches, *Archives of Computational Methods in Engineering*, Vol. 17, No.3, pp. 299-325.

Stavridis, A., and Shing, P . B. (2010). Finite Element Modeling of Nonlinear Behavior of Masonry-Infilled RC Frames, *Journal of Structural Engineering, ASCE, 136(3), 285-296.*, Vol. 3, No.136, pp. 285-296.

Tarque, N. (2011). Numerical modelling of the seismic behaviour of adobe buildings, *Ph.D. Thesis*, ROSE School, Istituto di Studi Superiori di Pavia IUSS, Pavia, Italy.

Wawrzynek, A., and Cincio, A. (2005). Plastic-damage macro-model for non-linear masonry structures subjected to cyclic or dynamic loads, *Proceedings of Conf. Analytical Models and New Concepts in Concrete and Masonry Structures, AMCM'2005*, Gliwice, Poland.